

the H₂BQ formation energy. The stability of the Mn-O bonds in the product is an important contributing factor to the calculated exothermicity. For the electronic structure of this complex a Mn 3d occupation of three unpaired electrons for Mn is assumed, which is suggested by the observation⁸ of a 3.3 μ_B magnetic moment.

Discussion and Conclusions

It was noted earlier that the photoactive Mn^{III} complexes all absorb at 590 nm and the inactive ones do not. Furthermore, the complex with highest activity, R = (CH₂)₃, showed the strongest 590-nm band. It is probable that this absorption is characteristic of dimerization. Electronic structures for our simplified H₂O-coordinated monomer and H₂O-bridged dimer are shown in Figure 7. It may be seen that the monomer Mn 3d set of orbitals is broadened by dimerization. The lowest ligand to Mn^{III} charge-transfer excitation is 0.6 eV less in energy in the dimer. Considering the approximations of our structural model for the dimer and the theoretical method, this corresponds well with the 0.8 eV difference between the first dimer peak and the first peak for the R = *o*-C₆H₄ monomer complex (~425 nm).^{8a} Furthermore, manipulations using structural models show that the dimer with R = (CH₂)₃ has less strain than the dimers with R = (CH₂)₂ and (CH₂)₄. In the inactive cases, where R = *o*-C₆H₄, CH₂, (CH₂)₅, and (CH₂)₆, strains appear to prevent dimerization. Therefore, it is suggested that the 590-nm band is symptomatic of dimerization of [LMn^{III}H₂O] monomers, and complexes that cannot dimerize cannot generate O₂ even if dehydrogenation and deprotonation of the H₂O in the monomer occurs. Oxidized Mn

monomers will suffer the same strains preventing dimerization.

H₂O bonded to Mn^{III} in the monomer or as bridges in the Mn^{III} dimer starts off the reaction sequence by transferring a hydrogen atom to an O⁻ created by a π*←n optical excitation in *p*-benzoquinone. This process oxidizes Mn^{III} to Mn^{IV} and creates tightly bound OH⁻ groups that are polarized sufficiently for easy deprotonation. It is the formation of the strong Mn-OH bond that prevents the formation of hydroxylated rings, as occurs in aqueous solution in the absence of the active Mn complexes.

The di-μ-oxo Mn^{IV} complex, which forms by either oxidation of the H₂O-bridged Mn^{III} dimer or by dimerization of oxidized monomers, cannot release O₂ because it is too stable. The energetics for a disproportionation process where two such dimers come together, and an O₂ molecule forms between them, leaving two [[LMn^{III}O]₂], seem feasible and, since all other steps are calculated to be downhill, this is probably the activation step.

The first-order dependence of the reaction rate on the concentration of the initial Mn^{III} complex is consistent with either monomer or dimer participation in the first step. The half-order dependence on *p*-benzoquinone concentration indicates that there are other reactions occurring.

Acknowledgment. Preparation of this manuscript was assisted by the donors of the Petroleum Research Fund, administered by the American Chemical Society. Md.K.A. is grateful for fellowship support from Tanta University.

Registry No. O₂, 7782-44-7; H₂O, 7732-18-5; [(H₂N)₂(OH)₂Mn^{III}H₂O]⁺, 117984-04-0; {[(H₂N)₂(OH)₂Mn^{III}H₂O]₂}²⁺, 117984-05-1; [LMn^{III}H₂O]⁺, 104494-13-5; *p*-benzoquinone, 106-51-4.

Reaction Ergodography for a Model of Siloxane Bond Formation in Organosilane Polymers

Akitomo Tachibana,*[†] Hiroyuki Fueno,[†] Yuzuru Kurosaki,[†] and Tokio Yamabe^{†,‡}

Contribution from the Department of Hydrocarbon Chemistry, Faculty of Engineering, Kyoto University, Kyoto 606, Japan. Received May 24, 1988

Abstract: Reaction ergodography using IRC (intrinsic reaction coordinate) as a unique reaction path is studied for a model of siloxane bond formation in organosilane polymers. This is a dehydrogenation reaction. Using a model system, we have obtained an activation energy of 44.2 kcal/mol and exothermicity of 17.4 kcal/mol (CISD+QC/6-31G**//RHF/3-21G^{*}). High reactivity of silicon is found as compared with the reactivity of carbon in an analogue reaction system with the activation energy of 129.2 kcal/mol and the endothermicity of 28.2 kcal/mol (CISD+QC/6-31G**//RHF/3-21G). The present dehydrogenation reaction scheme could be a candidate for a model of siloxane bond formation in organosilane polymers. This is consistent with the mechanism proposed by R. Withnal and L. Andrews (*J. Phys. Chem.* **1985**, 89, 3261).

I. Introduction

Photolysis of organosilane polymers has received much attention because of their characteristic sensitivity for UV irradiation. Corresponding interests have spread over wide fields of photoresists, photoinitiators for olefin polymerizations or precursors to β-SiC ceramics.^{1,2}

The origin for the intense reactivity of organosilane polymers has been shown to be due to the formation of silyl radicals and silylenes as the reaction intermediates. These will produce silylene insertion products and silyl radical derived products.² The evidence for the formation of photochemically generated silylene and silyl radicals has been confirmed by West et al. by using alcohol-containing solvents: silylene readily inserts into the oxygen-hydrogen bond, and silyl radicals readily abstract hydrogen radicals

and alkoxy radicals from alcohols.³

Photolysis of high molecular weight (PhMeSi)_n in degassed THF with excess Et₃SiH, however, leads to complex products such as Et₃SiO(PhMeSi)H, (Et₃Si)₂O, and H(PhMeSi)O(PhMeSi)H. The source of oxygen in these compounds is unknown. The mechanism for the formation of the siloxane bond Si-O-Si⁴⁻⁷ is

(1) See, for example: *Materials for Microlithography: Radiation-Sensitive Polymers*; Thompson, L., Wilson, C. G., Frecht, J. M. J., Eds.; American Chemical Society: Washington, DC, 1984. *Ultrastructure Processing of Ceramics, Glasses and Composites*; Heuch, L., Ulrich, D. R., Eds.; ACS Symposium Series 266; Wiley: New York, 1984.

(2) See, for example: Raabe, G.; Michl, J. *Chem. Rev.* **1985**, 85, 419.

(3) Trefonas, P., III; West, R.; Miller, R. D. *J. Am. Chem. Soc.* **1985**, 107, 2737.

(4) (a) Ruelle, P.; Nam-Tran, H.; Buchmann, M.; Kesselring, U. W.; *J. Mol. Struct. THEOCHEM* **1984**, 109, 177. (b) Chakoumakos, B. C.; Gibbs, G. V. *J. Phys. Chem.* **1986**, 90, 996. (c) Sauer, J.; Zurawski, B. *Chem. Phys. Lett.* **1979**, 65, 587. (d) Ernst, C. A.; Allred, A. L.; Ratner, M. A.; Newton, M. D.; Gibbs, G. V.; Moskowitz, J. W.; Topiol, S. *Chem. Phys. Lett.* **1981**, 81, 424. (e) Oberhammer, H.; Boggs, J. E. *J. Am. Chem. Soc.* **1980**, 102, 7241. (f) Grigoras, S.; Lane, T. H. *J. Comput. Chem.* **1987**, 8, 84.

[†] Also: Division of Molecular Engineering, Graduate School of Engineering, Kyoto University, Kyoto 606, Japan.

[‡] Also: Institute for Fundamental Chemistry, 34-4 Takano-Nishihiraki-cho, Sakyo-ku, Kyoto 606, Japan.

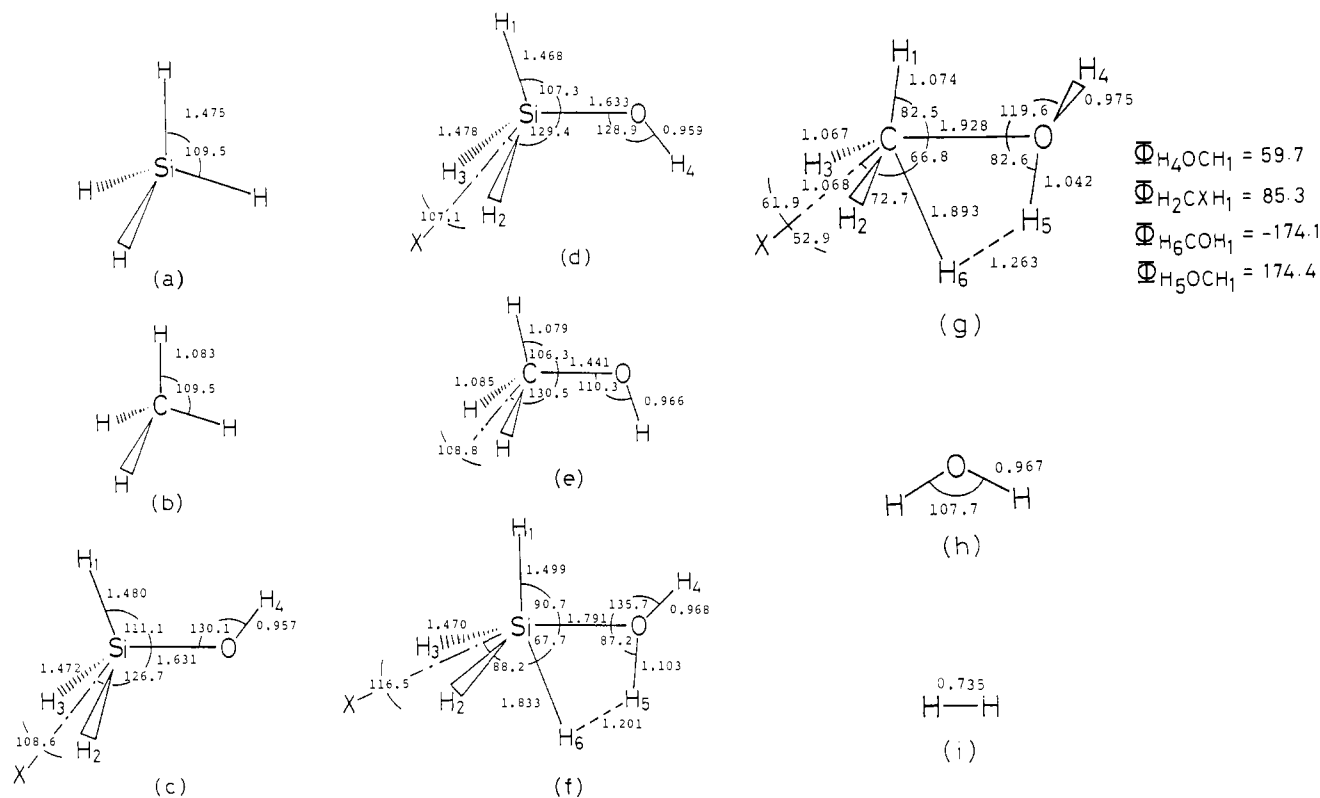
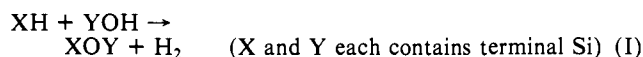


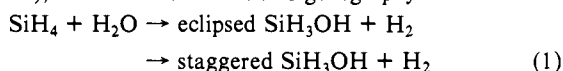
Figure 1. Optimized geometries of (a) SiH_4 , (b) CH_4 , (c) eclipsed SiH_3OH , (d) staggered SiH_3OH , (e) CH_3OH , (f) TS of reaction 1, (g) TS of reaction 2, (h) H_2O , and (i) H_2 . XSi bisects the angle $\angle\text{H}_2\text{SiH}_3$ and it is in the H_1SiO plane. XC is in the H_1CO plane and H_2CH_3 plane. Bond lengths and angles are given in Ångströms and degrees, respectively. The basis set is 3-21G(*).

also unknown, and it should be consistent with the mechanism of the formation of silylene or silyl radical.

To the resolution of these problems, we should find the ways through which (1) oxygen intrudes into the solution and (2) oxygen is trapped in the products. Then, one may assume that there may have been residual oxygen or water present in the solution, which terminates the radical chain reaction or scavenges the silylene, bringing about the terminal groups SiH and SiOH . Since the concentration of oxygen is assumed to be small, the possibility that more than two SiOH groups meet should be negligible. Then it follows that the following dehydrogenation reaction would be a candidate for the formation of the siloxane bond:



In the present paper, we have chosen a model system for reaction I. First, we have replaced X with H_3Si , and Y with H (reaction 1), and studied the reaction ergodography of this reaction



by using IRC (intrinsic reaction coordinate)⁸ as the unique reaction

(5) O'Keeffe, M.; Buseck, P. R. *Trans. Am. Crystallogr. Assoc.* **1979**, *15*, 27. Tossell, J. A. *Ibid.* **1979**, *15*, 47. O'Keeffe, M.; Hyde, B. G. *Ibid.* **1979**, *15*, 65. Tossell, J. A.; Lazzarotti, P. *Chem. Phys.* **1987**, *112*, 205. O'Keeffe, M.; Gibbs, G. V. *J. Chem. Phys.* **1984**, *81*, 876; *J. Phys. Chem.* **1985**, *89*, 4574. O'Keeffe, M.; McMillan, P. F. *Ibid.* **1986**, *90*, 541. Hess, A. C.; McMillan, P. F.; O'Keeffe, M. *Ibid.* **1986**, *90*, 5661. Hobza, P.; Sauer, J.; Morgener, C.; Hurych, J.; Zahradnik, R. *Ibid.* **1981**, *85*, 4061. Sauer, J.; Morgener, C.; Schröder, K.-P. *Ibid.* **1984**, *88*, 6375. Sauer, J.; Zahradnik, R. *Int. J. Quantum Chem.* **1984**, *26*, 793. Raghavachari, K.; Chandrasekhar, J.; Frisch, M. J. *J. Am. Chem. Soc.* **1982**, *104*, 3779.

(6) Almenningen, A.; Bastiansen, O.; Ewing, V.; Hedberg, K.; Traetteberg, M. *Acta Chem. Scand.* **1963**, *17*, 2455.

(7) Durig, J. R.; Flanagan, M. J.; Kalasinsky, V. F. *J. Chem. Phys.* **1977**, *66*, 2775.

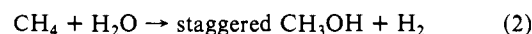
(8) Fukui, K. *J. Phys. Chem.* **1970**, *74*, 4161. Fukui, K.; Kato, S.; Fujimoto, H. *J. Am. Chem. Soc.* **1975**, *97*, 1. Ishida, K.; Morokuma, K.; Komornicki, A. *J. Chem. Phys.* **1977**, *66*, 2153. Miller, W. H.; Handy, N. C.; Adams, J. E. *Ibid.* **1980**, *72*, 99. Garret, B. C.; Truhlar, D. G.; Wagner, A. F.; Dunning, T. H., Jr. *Ibid.* **1980**, *73*, 2733.

Table I. Geometrical Parameters for XOY with X = H_3Si and Y = H

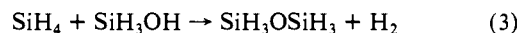
SiO, Å	OH, Å	$\angle\text{SiOH}$, deg	method
1.686	0.986	107.3	STO-3G ^a
1.64	0.94	134	6-31G(* ^b)
1.633	0.959	128.9	3-21G(* ^c)
1.647	0.946	119.0	6-31G* ^c

^aReference 4a. ^bReference 4b. ^cPresent work.

path. A reference analogue system, in which the Si is replaced with C (reaction 2) has also been treated in order for comparison



of reactivity. Second, we have chosen the simplest system for reaction I, namely, X and Y are both replaced with H_3Si (reaction 3). The energetics and the geometrical structure of the reaction



center at the transition state of reaction 3 have been found to be equivalent to those of reaction 1.

Reaction I itself has been proposed by Withnal and Andrews⁹ for the formation of disilyl ether in ozone photolysis experiments (see eq 16 in ref 9).

II. Methods of Calculation

The molecular orbital (MO) calculations were carried out with the GAUSSIAN-82¹⁰ program using the SCF method¹¹ with the 3-21G(*^{12a}) basis set for reactions 1-3. For reaction 3, they also were carried out with

(9) Withnal, R.; Andrews, L. *J. Phys. Chem.* **1985**, *89*, 3261.

(10) Binkley, J. S.; Frisch, M. J.; DeFrees, D. J.; Raghavachari, K.; Whiteside, R. A.; Schlegel, H. B.; Fluder, E. M.; Pople, J. A. *Gaussian 82, Release A version (Sept. 1983), An Ab Initio Molecular Orbital Program*; Carnegie Mellon University: Pittsburgh, PA, 1983.

(11) Roothaan, C. C. *J. Rev. Mod. Phys.* **1951**, *23*, 69.

(12) (a) Pietro, W. J.; Francl, M. M.; Hehre, W. J.; DeFrees, D. J.; Pople, J. A.; Binkley, J. S. *J. Am. Chem. Soc.* **1982**, *104*, 5039. (b) Francl, M. M.; Pietro, W. J.; Hehre, W. J.; Binkley, J. S.; Gordon, M. S.; DeFrees, D. J.; Pople, J. A. *J. Chem. Phys.* **1982**, *77*, 3654.

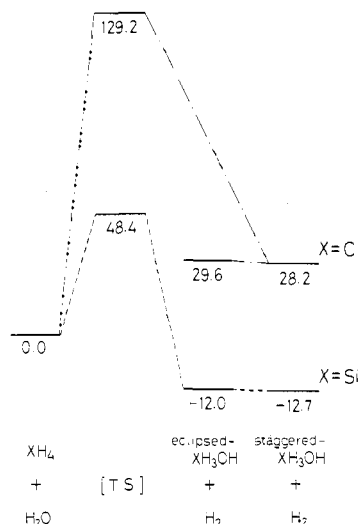


Figure 2. Relative energy values estimated by CISD+QC with the 6-31G** basis set. The geometries are the same as Figure 1. The units are kilocalories per mole.

the 6-31G*^{12b} basis set. Geometry optimization was performed by the use of the energy gradient method.¹³ The electron correlation energy for each geometry was estimated by single- and double-substituted configuration interaction (CISD)¹⁴ with the 6-31G**^{12b} basis set. The Davidson correction¹⁵ was added to allow for unlinked cluster quadruple correction (QC). The vibrational analysis was calculated by using the analytical second derivatives¹⁶ based on the SCF method. The IRC was calculated at the SCF level with the HONDOG¹⁷ program by the use of the 3-21G(*) basis set.

III. Results and Discussion

A. Geometries and Potential Energy Profiles of Reactions 1 and 2. The optimized geometries of reactions 1 and 2 are shown in Figure 1. We are interested in the XOY bond formation with X = H₃Si and Y = H. The relevant data in the literature are listed in Table I. The TSs were identified as the structure of a saddle point on the potential energy surface by vibrational analysis. The structure of reaction 1 has C_s symmetry and the reaction pathway 1 maintains C_s symmetry. The structure of TS of reaction 2 has C₁ symmetry, and so reaction 2 does not maintain C_s symmetry.

The relative energy values of optimized geometries are shown in Figure 2. X = Si shows reaction 1, and X = C shows reaction 2. The activation energy is 48.4 kcal/mol and the exothermic energy is 12.7 kcal/mol in reaction 1 (CISD+QC/6-31G**//RHF/3-21G(*)). The activation energy is 129.2 kcal/mol and the endothermic energy is 28.2 kcal/mol in reaction 2 (CISD+QC/6-31G**//RHF/3-21G). The reaction scheme of reaction 1 resembles that of reaction 2 and the difference is that the central atom of reaction 1 is silicon and that of reaction 2 is carbon. However, there is large difference in thermodynamical stability. The activation energy of reaction 1 is much smaller than that of reaction 2. Reaction 1 is exothermic, but on the other hand, reaction 2 is endothermic. Therefore, reaction 1 occurs more easily than reaction 2.

In Figure 3 are shown the potential energy profiles for reactions 1 and 2. The abscissa is the IRC,⁸ the origin corresponds to the TS, the negative side corresponds to the reactant region, and the positive side corresponds to the product region. The net charges of the TSs are shown in Figure 4a,b. The net charge of the silicon atom is positive and that of the carbon atom is negative. Both

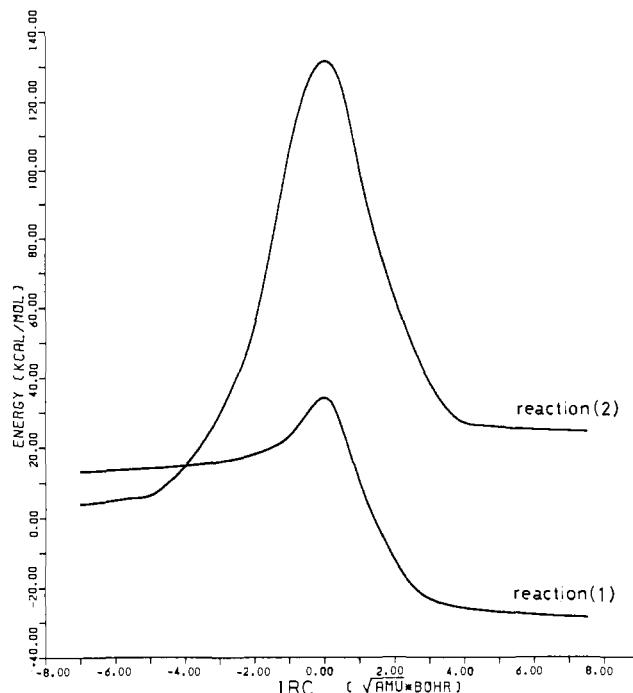


Figure 3. Potential energy profile along the IRC for reaction 1 and reaction 2.

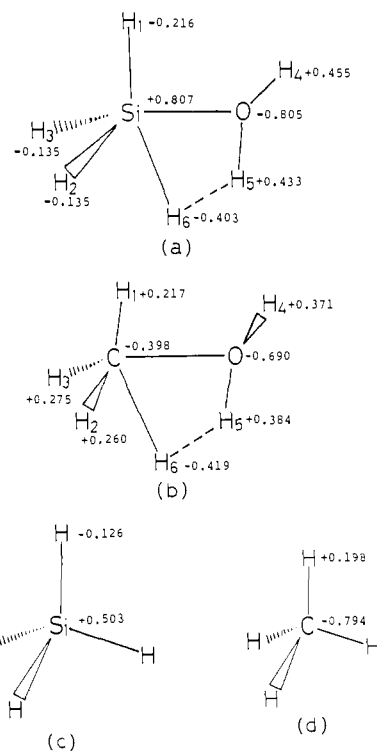


Figure 4. Net charges of (a) TS of reaction 1, (b) TS of reaction 2, (c) SiH₄, and (d) CH₄.

of the net charges of the oxygen atom are negative. The charges of H4 are positive for both reaction 1 and reaction 2. But the charge of H1 is negative for reaction 1 and positive for reaction 2. Therefore, the H1-H4 interaction of reaction 1 is attractive and that of reaction 2 is repulsive. This may make it easier for H4 of reaction 1 to be out of the H1CO plane. The geometry changes along the IRC of reaction 1 are shown in Figure 5. The SiO bond distance of TS is 1.791 Å and that of eclipsed silanol is 1.631 Å. The CO bond distance of TS is 1.928 Å and that of methanol is 1.441 Å. It is worth noting in the changes of bond length as shown in Figure 5a that the cleavage of the SiH6 bond and OH5 bond occurs from TS and the formation of the SiO bond

(13) Pulay, P. In *Modern Theoretical Chemistry*; Schaefer, H. F., III, Ed.; Plenum: New York, 1977; Vol. 4, Chapter 4.

(14) Pople, J. A.; Binkley, J. S.; Seeger, R. *Int. J. Quantum Chem.* **1976**, *S10*, 1.

(15) (a) Langhoff, S. R.; Davidson, E. R. *Int. J. Quantum Chem.* **1974**, *8*, 61. (b) Davidson, E. R.; Silver, D. W. *Chem. Phys. Lett.* **1978**, *52*, 403.

(16) Pople, J. A.; Krishnan, R.; Schlegel, H. B.; Binkley, J. S. *Int. J. Quantum Chem.* **1979**, *S13*, 225.

(17) Dupuis, M.; King, H. F. *J. Chem. Phys.* **1978**, *68*, 3998.

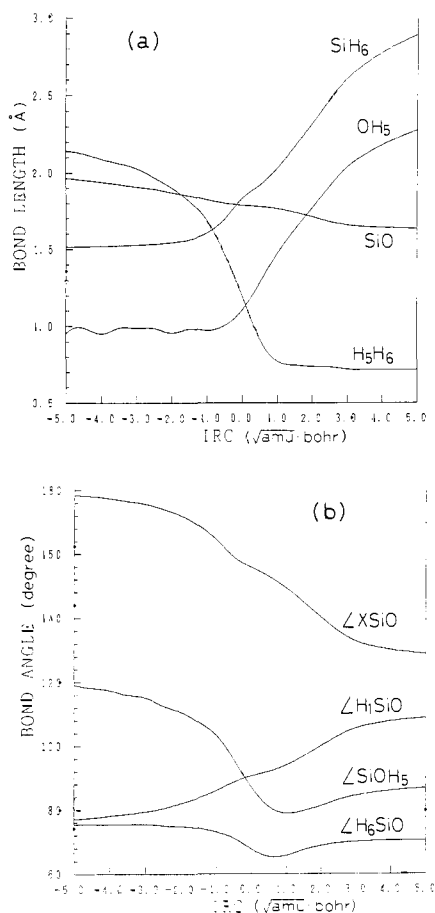


Figure 5. Geometrical parameters along IRC of reaction 1: (a) bond lengths and (b) bond angles.

Table II. Geometrical Parameters for XOY with X = Y = H₃Si

SiO, Å	$\angle \text{SiOSi}$, deg	method
1.658	124.0	STO-3G ^a
1.636	180.0	4-31G ^b
1.634	142	DZ+d effective potentials ^c
1.617	143.3	3-3-21* for Si and 4-21* for O ^d
1.645	149.5	3-21G* ^e
1.634	144.1	experiment ^f
	149	experiment ^g
1.627	180.0	3-21G(*) ^h
1.627	166.0	6-31G* ^h

^aReference 4a. ^bReference 4c. ^cReference 4d. ^dReference 4e. ^eReference 4f. ^fReference 6. ^gReference 7. ^hPresent work.

and H₅H₆ bond has made progress before TS. These decrease the barrier height of TS. It is noteworthy in the changes of bond angle as shown in Figure 5b that the hollows for changes of $\angle \text{SiOH}_5$ and $\angle \text{H}_6\text{SiO}$ appear around TS. This indicates the action that make H₅ and H₆ come close. It makes the formation of the H₅H₆ bond and the dissociation of H₂ easy.

B. Geometries and Potential Energy Profiles for Reaction 3.

The optimized geometries of reaction 3 with 6-31G* are shown in Figure 6. The geometrical parameters in Figure 1, parts a, c, d, and i, are here updated as follows. The SiH bond length of silane is 1.475 Å. For eclipsed silanol, the bond lengths, SiO, SiH₁, SiH₂, and OH₄ are 1.648, 1.479, 1.473, and 0.945 Å, respectively, and the bond angles, $\angle \text{H}_1\text{SiO}$, $\angle \text{XSiO}$, $\angle \text{H}_2\text{SiH}_3$, and $\angle \text{SiOH}_4$ are 109.9, 126.2, 108.7, and 119.0°, respectively. For staggered silanol, the bond lengths, SiO, SiH₁, SiH₂, and OH₄ are 1.647, 1.469, 1.478, and 0.946 Å, respectively, and the bond angles, $\angle \text{H}_1\text{SiO}$, $\angle \text{XSiO}$, $\angle \text{H}_2\text{SiH}_3$, and $\angle \text{SiOH}_4$ are 106.9, 128.3, 107.7, and 119.0°, respectively. The bond length of H₂ is 0.730 Å; $\angle \text{SiOSi}$ of disiloxane is 166.0°, as shown in Figure 6c. This angle varies depending on experiments, 144.1⁶ or 149°,⁷ and on calculational methods,⁴ as summarized in Table II. It

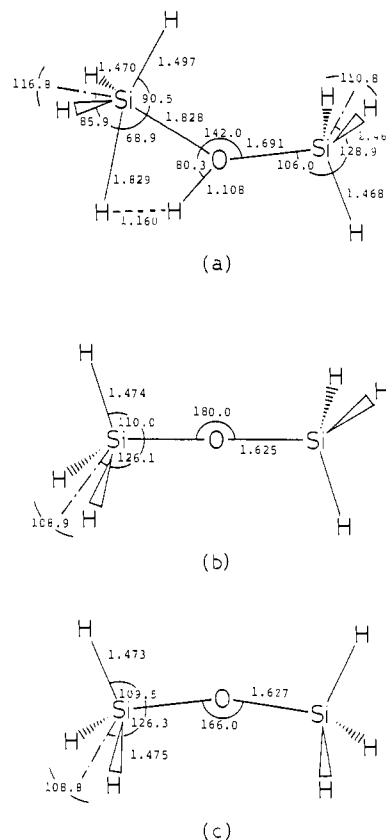


Figure 6. Optimized geometries of (a) TS of reaction 3, (b) disiloxane (D_{3d}), and (c) disiloxane (C_{2v}). Bond lengths and angles are given in Ångströms and degrees, respectively. The basis set is 6-31G*.

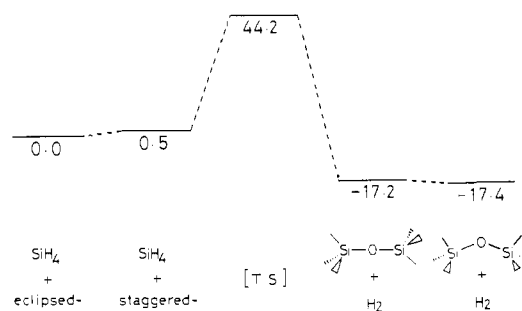


Figure 7. Relative energy values estimated by CISD+QC with the 6-31G** basis set. The geometries are the same as in Figure 6. The units are kilocalories per mole.

is 180.0° by use of the 3-21G(*) basis set. In order to obtain a theoretical value closer to the experimental value, the 6-31G* basis set was used. The TS has C_s symmetry. Disiloxane (D_{3d}) has one imaginary vibrational frequency corresponding to the rotation of SiH₃ around the SiOSi axis. After the rotation of SiH₃, disiloxane (C_{2v}) is obtained. The relative energy values are shown in Figure 7.

The activation energy of reaction 3, 44.2 kcal/mol, is almost equal to that of reaction 1, 48.4 kcal/mol. The exothermicity of reaction 3, 17.4 kcal/mol, is close to that of reaction 1, 12.7 kcal/mol. The reaction center is a four-atom system, Si-O-H-H, in both reactions 1 and 3. Bond lengths, SiO, SiH, OH, and HH for reaction 1 are 1.791, 1.833, 1.103, and 1.201 Å, as shown in Figure 1f, and for reaction 3 are 1.828, 1.829, 1.108, and 1.160 Å, as shown in Figure 6a, respectively. And so, the geometry of TS for reaction 3 is very similar to the geometry of TS for reaction 1. These results indicate that reaction 3 is analogous to reaction 1. Then, it can be considered that the formation of the siloxane bond between silicon compounds that have higher molecular weights occurs similarly. The present dehydrogenation reaction scheme could be a candidate for a model of siloxane bond for-

mation in organosilane polymers.

IV. Concluding Remarks

The experimentally unknown mechanism for the formation of the siloxane bond in radiated organosilane polymer solutions has been examined. We have assumed that the residual oxygen or water should be present in the solution, which terminates the radical chain reaction or scavenges the silylene, bringing about the terminal groups SiH and SiOH. Then it follows that the dehydrogenation reaction I would be a candidate for the formation of the siloxane bond, which is studied numerically by using ab initio MO theory. Our computed activation energies for the reactions involving silicon are seen to be lower than those for analogous reactions of carbon by a factor of about $2/3$, as is often the case. In particular, our relatively low activation energy for

siloxane formation, 44.2 kcal/mol, supports the Withnal and Andrews reaction scheme.⁹ Reaction ergodography for the model reaction system is also examined in order to characterize the course of the reaction pathway.

Acknowledgment. This work was supported by a Grant-in-Aid for Scientific Research from the Ministry of Education, Science and Culture of Japan, for which we express our gratitude. The numerical calculations were carried out at the Data Processing Center of Kyoto University and the Computer Center of the Institute for Molecular Science (IMS), who are thanked for their generous permission to use the FACOM M-780 and VP-400E and HITAC M-680H and S-820 computer systems, respectively.

Registry No. SiH₄, 7803-62-5; H₂O, 7732-18-5; SiH₃OH, 14475-38-8; SiH₃OSiH₃, 13597-73-4.

Superdense Carbon, C₈: Supercubane or Analogue of γ -Si?

Roy L. Johnston[†] and Roald Hoffmann*

Contribution from the Department of Chemistry and Materials Science Center, Cornell University, Ithaca, New York 14853-1301. Received June 27, 1988

Abstract: A new crystalline allotrope of carbon, "C₈", which is denser than diamond, has recently been claimed, following research on the plasma deposition of thin carbon films. The reported structure consists of a body-centered cubic array of C₈ cubes, forming a lattice previously postulated by Burdett and termed "supercubane". Discrepancies in the crystallographic analysis and the unusual bond length distribution in the reported structure lead us, however, to doubt the validity of the proposed structure of C₈. We have found, by means of a structural analysis combined with extended Hückel band calculations, that a likely alternative structure for C₈ is the BC-8 structure adopted by the high-pressure γ -Si allotrope. Our calculations indicate that this allotrope of carbon should have a small direct band gap at point H in the Brillouin zone, though a slight structural distortion leads to an increase in the gap. The small band gap is associated with a relatively short (2.18 Å) nonbonded C---C contact in the BC-8 structure. Finally, the BC-8 structure has been compared to a polymer of [1.1.1]propellane.

Diamondlike Films and Hypothetical Carbon Allotropes. In recent years the synthesis and study of "diamondlike" films has become a popular field for chemists, physicists, and materials scientists.¹⁻⁵ The term diamondlike generally implies a similarity in structure (i.e. most or all of the carbon atoms are bonded to four others in an approximately tetrahedral fashion), as well as physical properties, to diamond. The properties of diamond that make the synthesis of these films so attractive are its supreme hardness, chemical inertness, high electrical resistivity, and extremely high thermal conductivity. Advances in thin-film technology⁵ mean that it is possible to synthesize diamondlike materials with relatively large surface areas for application in the fields of mechanical engineering and electronics.^{1b}

The most common methods of generating thin diamondlike films are chemical vapor deposition and ion-beam/plasma deposition of carbon atoms, ions, or molecules generated by pyrolysis, sputtering, electrical discharge, etc., of hydrocarbon or carbon (e.g. graphite) starting materials.^{1a,3} The resulting films are usually amorphous, sometimes contain hydrogen, and often possess a mixture of sp³ and sp² carbon (i.e. 4- and 3-connected atoms). Excellent reviews of the field are to be found in the papers of DeVries,^{1a,2} Angus,⁴ and Weissmantel.⁵

Diamondlike films are generally regarded as metastable,^{1a} since the conditions under which they are synthesized are far removed from those (high static pressure and temperature) under which diamond is thermodynamically stable.⁶ In the case of ion-beam and plasma deposition synthesis, the formation of metastable phases has been attributed to the extremely rapid collapse (over

a time scale of around 10⁻¹¹ s) of localized (approx. 20 Å radius) thermal spikes caused by the ion/atom impinging on the growing carbon film. In these spikes, the nonequilibrium temperatures (10³-10⁴ K) and pressures (around 10 GPa) can be very high.^{3,7}

As mentioned above, diamondlike films are generally amorphous (i.e. possess no long-range order). While the theory of amorphous phases is a fascinating subject,⁸⁻¹¹ there is a certain aesthetic appeal to crystalline matter. In particular, there has been much interest in postulating structures for (and predicting electronic properties of) novel crystalline allotropes of carbon,^{12,13} and over the years

(1) (a) For an excellent, thorough historical account of the field, see: DeVries, R. C. *Annu. Rev. Mater. Sci.* **1987**, *17*, 161. (b) A less comprehensive, though quite readable, account can be found in: Simpson, M. *Materials with the Diamond Touch*. *New Scientist* **1988**, No. 1603, 50.

(2) Badzian, A. R.; DeVries, R. C. *Mater. Res. Bull.* **1988**, *23*, 385.

(3) Klabunde, K. J., Ed. *Thin Films from Free Atoms and Particles*; Academic Press: New York, 1985.

(4) (a) Angus, J. C. *Thin Solid Films* **1986**, *142*, 145. (b) Angus, J. C.; Jansen, F. J. *Vac. Sci. Technol.* **1988**, *A6*, 1778. (c) Angus, J. C.; Hayman, C. C. *Science* **1988**, *241*, 913.

(5) (a) Weissmantel, C.; Breuer, K.; Winde, B. *Thin Solid Films* **1983**, *100*, 383. (b) Weissmantel, C. In Reference 3; Chapter 4, p 153.

(6) For a discussion of the phase diagram of elemental carbon, see: Bundy, F. P. *J. Geophys. Res.* **1980**, *85*, 6930.

(7) Rabelais, J. W.; Kasi, S. *Science* **1988**, *239*, 623.

(8) Brodsky, M. H., Ed. *Amorphous Semiconductors (Top. Appl. Phys. Vol. 36)*; Verlag: Berlin, 1985.

(9) Bicerano, J.; Adler, D. *Pure Appl. Chem.* **1987**, *59*, 102.

(10) Joannopoulos, J. D.; Cohen, M. L. *Solid State Phys.* **1976**, *31*, 71.

(11) Robertson, J.; O'Reilly, E. P. *Phys. Rev. B* **1987**, *35*, 2946.

(12) (a) Balaban, A. T.; Rentia, C. C.; Cuiipitu, E. *Rev. Roum. Chim.* **1968**, *13*, 231. (b) Baughman, R. H.; Eckhardt, H.; Kertesz, M. *J. Chem. Phys.* **1987**, *87*, 6687.

[†]SERC/NATO Postdoctoral Fellow 1987-1988.